

# Solution Structure and Behavior of Dimeric Uranium(III) Metallocene Halides

Wayne W. Lukens, Jr., Sharon M. Beshouri, Anthony L. Stuart, and Richard A. Andersen\*

Chemistry Department and Chemical Sciences Division of Lawrence Berkeley Laboratory, University of California, Berkeley, California 94720

Received July 14, 1998

The variable-temperature  $^1\text{H}$  NMR behavior of the uranium(III) dimers  $[\text{Cp}''_2\text{UX}]_2$  and  $[\text{Cp}^+_2\text{UX}]_2$ , where X is F, Cl, Br, or I,  $\text{Cp}''$  is 1,3-( $\text{Me}_3\text{Si}$ ) $_2\text{C}_5\text{H}_3$ , and  $\text{Cp}^+$  is 1,3-( $\text{Me}_3\text{C}$ ) $_2\text{C}_5\text{H}_3$ , has been examined. At low temperature, the number of inequivalent  $\text{CMe}_3$  or  $\text{SiMe}_3$  groups implies that the solution structure is the same as the solid-state structure in all of these complexes. The barriers to ring rotation in the  $\text{Cp}''$  series are strongly dependent upon the U–X distance, but all of the barriers to ring rotation in the  $\text{Cp}^+$  series are the same. The trends in ring rotation barriers are explained by the different conformations of the Cp ligands in the dimers. In addition to the homo-halide dimers, the variable-temperature NMR behavior of the hetero-halide dimers  $\text{Cp}'_4\text{U}_2(\mu\text{-X})(\mu\text{-Y})$ , where  $\text{Cp}'$  is  $\text{Cp}''$  or  $\text{Cp}^+$  and X and Y are halides where  $\text{X} \neq \text{Y}$ , was examined. Above room temperature, the halide atoms exchange sites rapidly on the NMR time scale.

## Introduction

The metallocene chemistry of trivalent uranium is based largely upon tris(cyclopentadienyl) complexes of the type  $\text{Cp}'_3\text{U}$  or  $\text{Cp}'_3\text{U(L)}$ , where  $\text{Cp}'$  is  $\text{C}_5\text{H}_5$  or a substituted cyclopentadienyl ligand and L is a Lewis base.<sup>1,2</sup> Complexes with only two cyclopentadienyl rings on the uranium,  $\text{Cp}'_2\text{UX}$ , cannot be isolated in pure form unless the cyclopentadienyl group contains sterically demanding substituents. The bulky rings prevent ligand redistribution by stabilizing  $\text{Cp}'_2\text{UX}$  relative to  $\text{Cp}'_3\text{U}$ . Devising strategies for preparing redistribution-stabilized metallocenes of trivalent uranium is likely to be rewarding, since the insertion and oxidation reactions are likely to be extensive.<sup>3</sup>

In comparison to the chemistry of  $\text{Cp}'_3\text{U(L)}$ , the chemistry of  $\text{Cp}'_2\text{UX}$  complexes has not been as extensively explored. Trimeric  $[(\text{Me}_3\text{C}_5)_2\text{UCl}]_3$  is sparingly soluble in toluene,<sup>4</sup> and its chloride bridges can be cleaved by two-electron donors such as tetrahydrofuran and sodium chloride.<sup>4,5</sup> The only other known dicyclopentadienyl complexes of U(III) are the dimers  $[1,3-(\text{Me}_3\text{Si})_2\text{C}_5\text{H}_3]_4\text{U}_2(\mu\text{-X})_2$ .<sup>6,7</sup> These hexane-soluble com-

plexes have been characterized in the solid state for X = Cl and Br. These dimers and their  $\text{Me}_3\text{C}$  analogues  $[1,3-(\text{Me}_3\text{C})_2\text{C}_5\text{H}_3]_4\text{U}_2(\mu\text{-X})_2$ <sup>8</sup> should be useful synthons for further synthetic reactions. In addition, their high solubility in hydrocarbon solvents offers the opportunity for studying ligand exchange reactions and fluxional processes, provided that ring redistribution reactions are slow. In this paper we describe our synthetic and  $^1\text{H}$  NMR solution studies on the dimers  $(1,3\text{-R}_2\text{C}_5\text{H}_3)_4\text{U}_2(\mu\text{-X})_2$ , where X is a halide and R is  $\text{SiMe}_3$  ( $\text{Cp}''$ ) or  $\text{CMe}_3$  ( $\text{Cp}^+$ ).

## Results

**Synthesis and Physical Properties.** The most convenient synthesis of the trivalent metallocene dimers is the reaction of the tetravalent metallocene dihalides<sup>9</sup> with *t*-BuLi in hexane, since all of the reactants and all of the products except for  $[\text{Cp}^+_2\text{UF}]_2$  are hexane-soluble. Alternative synthetic routes using sodium amalgam have been used by Lappert to prepare the series  $[\text{Cp}''_2\text{-UX}]_2$ , for X = F, Cl, Br, and I. The reduction with *t*-BuLi most likely proceeds via a U(IV) *tert*-butyl species that undergoes homolytic cleavage of the weak U–C bond to give the trivalent metallocene and a *tert*-butyl radical. A similar radical process has been observed in the reactions of  $\text{Cp}'_3\text{UCMe}_3$ .<sup>10</sup> All of the dimers are green and crystallize from hexane, except for  $[\text{Cp}^+_2\text{UF}]_2$ , which was crystallized from toluene. All of the complexes have high melting points and give dimeric molecular ions in their electron ionization mass spectra, except  $\text{Cp}^+_2\text{UI}$  and  $\text{Cp}^+_2\text{UBr}$ , which give monomeric molecular ions.

\* To whom correspondence should be addressed at the Chemistry Department, University of California.

(1) (a) Kanellakopoulos, B.; Fischer, E. O.; Dornberger, E.; Baumgartner, F. *J. Organomet. Chem.* **1970**, *24*, 507. (b) Wasserman, H. J.; Zozulin, A. J.; Moody, D. C.; Ryan, R. R.; Salazar, K. V. *J. Organomet. Chem.* **1983**, *254*, 305.

(2) Santos, I.; Peres de Matos, A.; Maddock, A. G. *Adv. Inorg. Chem.* **1989**, *34*, 65.

(3) Lukens, W. W., Jr.; Beshouri, S. M.; Blosch, L. L.; Andersen, R. A. *J. Am. Chem. Soc.* **1996**, *118*, 901–902.

(4) Fagan, P. J.; Manriquez, J. M.; Marks, T. J.; Day, C. S.; Vollmer, S. H.; Day, V. W. *Organometallics* **1982**, *1*, 170–180.

(5) Finke, R. G.; Hirose, Y.; Gaughan, G. *J. Chem. Soc., Chem. Commun.* **1981**, 232.

(6) Blake, P. C.; Lappert, M. F.; Taylor, R. G.; Atwood, J. L.; Hunter, W. E.; Zhang, H. *J. Chem. Soc., Chem. Commun.* **1986**, 1394–1395.

(7) Blake, P. C.; Lappert, M. F.; Taylor, R. G.; Atwood, J. L.; Zhang, H. *Inorg. Chim. Acta* **1987**, *129*, 12–20.

(8) Zalkin, A.; Stuart, A. L.; Andersen, R. A. *Acta Crystallogr.* **1988**, *C44*, 2106–2108.

(9) Lukens, W. W., Jr.; Beshouri, S. M.; Blosch, L. L.; Stuart, A. L.; Andersen, R. A. *Organometallics* **1999**, *18*, 1235–1246.

(10) Weydert, M.; Brennan, J. G.; Andersen, R. A.; Bergman, R. G. *Organometallics* **1995**, *14*, 3942.

**Table 1.**  $^1\text{H}$  NMR Chemical Shifts of U(III) Halide Dimers at 30 °C in Benzene- $d_6$ <sup>a</sup>

compd	$\delta(\text{Me}_3\text{X})$ (X = C, Si)	$\delta(\text{A}_2)$	$\delta(\text{B})$
$[\text{Cp}^{\ddagger}_2\text{UF}]_2$	-11.78(51)		
$[\text{Cp}^{\ddagger}_2\text{UCl}]_2$	-6.66(36)	-51.62(400)	61.98(400)
$[\text{Cp}^{\ddagger}_2\text{UBr}]_2$	-5.37(34)	-62.77(200)	76.64(300)
$[\text{Cp}^{\ddagger}_2\text{UI}]_2$	-4.32(38)	-68.5(250)	86.9(400)
$[\text{Cp}^{\prime\prime}_2\text{UF}]_2$	-10.84(28)		
$[\text{Cp}^{\prime\prime}_2\text{UCl}]_2$	-9.01(11)	-2.61(140)	29.76(190)
$[\text{Cp}^{\prime\prime}_2\text{UBr}]_2$	-8.30(13)	-5.09(160)	35.49(120)
$[\text{Cp}^{\prime\prime}_2\text{UI}]_2$	-7.08(15)	-3.17(140)	41.62(170)

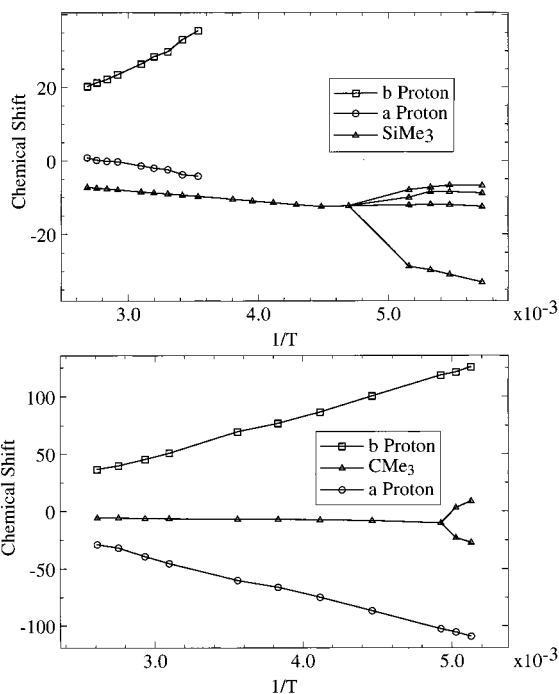
<sup>a</sup> The fwhm of each resonance, in units of Hz, is given in parentheses.

The chemical shifts of the protons of the complexes at 30 °C are given in Table 1. All of the chemically distinct resonances are observed, and they are assigned by integration. The  $\text{Me}_3\text{Si}$  or  $\text{Me}_3\text{C}$  resonances are slightly broader than the equivalent resonances in the U(IV) metallocene dihalides, and the  $\text{A}_2$  and B methine protons of the cyclopentadienyl ring are an order of magnitude broader than in the U(IV) complexes.<sup>9</sup> An exception is that the  $\text{A}_2$  and B proton resonances of the fluoride dimers are too broad to observe at all temperatures studied, even though the  $\text{Me}_3\text{Si}$  or  $\text{Me}_3\text{C}$  resonances are not appreciably broadened. The line width trend has been noted previously.<sup>11</sup> As noted in the metallocene U(IV) dihalides, the chemical shift of the  $\text{A}_2$  protons moves upfield ( $\delta < 0$ ), and that of the B proton moves in the opposite way ( $\delta > 0$ ), relative to the  $\text{Me}_3\text{E}$  resonance, and the relative shifts depend on the identity of the bridging ligands. Unfortunately, the ring resonances cannot be observed for the fluorides; therefore, the trend is not so striking as it is in the U(IV) dihalides. In addition to the room-temperature spectra, the variable-temperature spectra were obtained from -90 to 100 °C in toluene- $d_8$ . These data are conveniently displayed in graphical form, and plots of the chemical shifts of the protons of  $[\text{Cp}^{\prime\prime}_2\text{UCl}]_2$  and  $[\text{Cp}^{\ddagger}_2\text{UCl}]_2$  against inverse absolute temperature are shown in Figure 1. In the series  $[\text{Cp}^{\ddagger}_2\text{UX}]_2$ , where X is Cl, Br, or I, two inequivalent sets of  $\text{CMe}_3$  groups are present at low temperature. In the  $[\text{Cp}^{\ddagger}_2\text{UX}]_2$  series when X is Cl or Br, four inequivalent sets of  $\text{SiMe}_3$  groups are observed at low temperature, and the barrier to site exchange was calculated using the chemical shifts of the two sets of protons with the greatest difference in chemical shift. For  $[\text{Cp}^{\prime\prime}_2\text{UI}]_2$ , no low-temperature limiting spectrum was obtained. The low-temperature limiting spectra of the fluorides were different from those of the other halides. Only two sets of inequivalent  $\text{SiMe}_3$  groups are observed for  $[\text{Cp}^{\prime\prime}_2\text{UF}]_2$ , but six sets of inequivalent  $\text{CMe}_3$  groups are observed for  $[\text{Cp}^{\ddagger}_2\text{UF}]_2$  below -30 °C. The barriers to site exchange of the  $\text{CMe}_3$  or  $\text{SiMe}_3$  groups, "ring rotations", in these homo-bridged dimers are given in Table 2. The term "ring rotation" is set in quotation marks since complete rotation about the pseudo- $\text{C}_5$  axis of the Cp ligand is not necessary to account for site exchange; oscillation about this axis can also result in site exchange. The barrier was calculated

(11) Brennan, J. G.; Andersen, R. A.; Zalkin, A. *Inorg. Chem.* **1986**, 25, 1756.

(12) Luke, W. D.; Streitwieser, A., Jr. *J. Am. Chem. Soc.* **1981**, 103, 3241.

(13) Sandström, J. *Dynamic NMR Spectroscopy*; Academic Press: London, 1982.

**Figure 1.** Chemical shifts of the protons of  $[\text{Cp}^{\prime\prime}_2\text{UCl}]_2$  (upper) and  $[\text{Cp}^{\ddagger}_2\text{UCl}]_2$  (lower) versus temperature.**Table 2. Barriers to Ring Substituent Site Exchange in Dicyclopentadienyluranium(III) Halides**

	barrier <sup>a</sup>	$T_c$ <sup>b</sup>		barrier <sup>a</sup>	$T_c$ <sup>b</sup>
$[\text{Cp}^{\prime\prime}_2\text{UF}]_2$	12.4	-2	$[\text{Cp}^{\ddagger}_2\text{UF}]_2$	13.5	30
$[\text{Cp}^{\prime\prime}_2\text{UCl}]_2$	8.9 <sup>c</sup>	-60	$[\text{Cp}^{\ddagger}_2\text{UCl}]_2$	8.2	-70
$[\text{Cp}^{\prime\prime}_2\text{UBr}]_2$	7.9 <sup>c</sup>	-80	$[\text{Cp}^{\ddagger}_2\text{UBr}]_2$	8.9	-52
$[\text{Cp}^{\prime\prime}_2\text{UI}]_2$		< -95	$[\text{Cp}^{\ddagger}_2\text{UI}]_2$	8.9	-50

<sup>a</sup> In kcal mol<sup>-1</sup>. <sup>b</sup> In °C. <sup>c</sup> For  $[\text{Cp}^{\prime\prime}_2\text{UBr}]_2$  and  $[\text{Cp}^{\prime\prime}_2\text{UCl}]_2$ , the barrier was calculated using the two resonances with the greatest chemical shift difference of the four inequivalent  $\text{SiMe}_3$  resonances.

using the chemical shifts extrapolated to the coalescence temperature, since the chemical shifts vary with temperature.<sup>12,13</sup>

In addition to the homo-halide dimers, the NMR behavior of the hetero-halide dimers  $\text{Cp}'_4\text{U}_2(\mu\text{-X})(\mu\text{-Y})$  was examined. These species cannot be isolated, since they are obtained as a statistical mixture along with the two homo-bridged dimers by mixing the homo-dimers in toluene- $d_8$ . The equilibration is rapid and is complete within a few minutes at room temperature. The  $^1\text{H}$  NMR spectrum of the solution showed two new A protons, two new  $\text{SiMe}_3$  or  $\text{CMe}_3$  peaks, and a new B peak in addition to the resonances due to the homo-dimers. When equal amounts of starting halide dimers were used, all of the resonances had approximately the same area; the peaks are difficult to integrate since they overlap. Mixing varying amounts of the homo-dimers allows the individual resonances to be assigned with certainty. The new peaks are presumably due to a single dimer in which the bridging halides are different. In such a complex, the A protons and the  $\text{SiMe}_3$  or  $\text{CMe}_3$  groups are diastereotopic, which explains why two resonances are observed for the A and the  $\text{SiMe}_3$  or  $\text{CMe}_3$  protons.

The variable-temperature  $^1\text{H}$  NMR spectra of these mixtures were also examined. Plots of the chemical shift against inverse absolute temperature are shown in

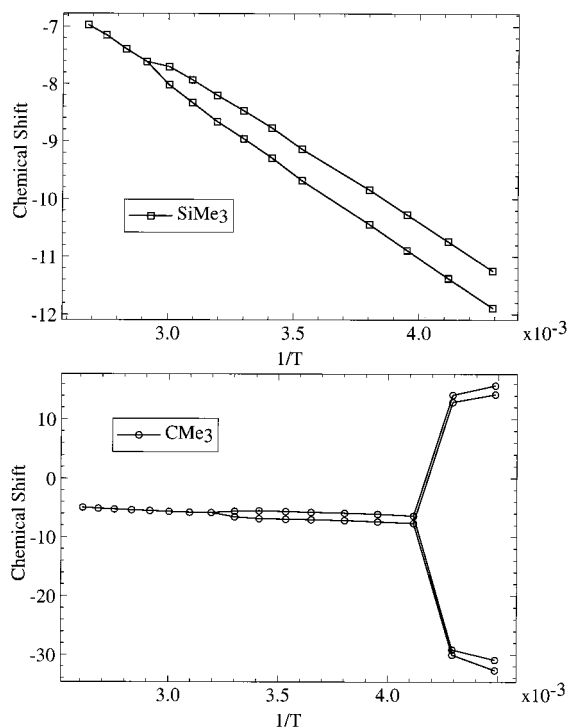


**Figure 2.** Chemical shifts of the SiMe<sub>3</sub> protons of Cp''<sub>4</sub>U<sub>2</sub>(μ-Cl)(μ-Br) (upper) and of the CMe<sub>3</sub> protons of Cp<sup>+</sup><sub>4</sub>U<sub>2</sub>(μ-Cl)(μ-Br) (lower) versus temperature.

**Table 3. Barriers to Ring Substituent Site Exchange in Dicyclopentadienyluranium(III) Hetero-Halides**

	barrier <sup>a</sup>	T <sub>c</sub> <sup>b</sup>		barrier <sup>a</sup>	T <sub>c</sub> <sup>b</sup>
Cp'' <sub>4</sub> U <sub>2</sub> (μ-Br,μ-F)	11.0	-10	Cp <sup>+</sup> <sub>4</sub> U <sub>2</sub> (μ-Br,μ-Cl)	9.0	-50
Cp'' <sub>4</sub> U <sub>2</sub> (μ-I,μ-F)	9.9	-30	Cp <sup>+</sup> <sub>4</sub> U <sub>2</sub> (μ-Br,μ-I)	9.2	-50
			Cp <sup>+</sup> <sub>4</sub> U <sub>2</sub> (μ-I,μ-Cl)	8.7	-50

<sup>a</sup> In kcal mol<sup>-1</sup>. <sup>b</sup> In °C.

**Table 4. Barriers to the Coalescence of the Diastereotopic Protons in Cp<sup>+</sup><sub>4</sub>U<sub>2</sub>(μ-X)(μ-Y)**

	CMe <sub>3</sub> proton				a <sub>2</sub> proton			
	X = Cl		X = Br		X = Br		X = Br	
	barrier <sup>a</sup>	T <sub>c</sub> <sup>b</sup>	barrier <sup>a</sup>	T <sub>c</sub> <sup>b</sup>	barrier <sup>a</sup>	T <sub>c</sub> <sup>b</sup>	barrier <sup>a</sup>	T <sub>c</sub> <sup>b</sup>
Y = Br	15.0	40			15.2	60		
Y = I	13.6	30	13.6	20	13.7	50	13.7	40

<sup>a</sup> In kcal mol<sup>-1</sup>. <sup>b</sup> In °C.

**Table 5. Barriers to the Coalescence of the Diastereotopic SiMe<sub>3</sub> Protons in Cp''<sub>4</sub>U<sub>2</sub>(μ-X)(μ-Y)**

	X = F		X = Cl		X = Br	
	barrier <sup>a</sup>	T <sub>c</sub> <sup>b</sup>	barrier <sup>a</sup>	T <sub>c</sub> <sup>b</sup>	barrier <sup>a</sup>	T <sub>c</sub> <sup>b</sup>
	Y = Br	15.7	50	16.7	70	
Y = I	15.6	40	16.2	70	16.0	60

<sup>a</sup> In kcal mol<sup>-1</sup>. <sup>b</sup> In °C.

Figure 2 for Cp''<sub>4</sub>U<sub>2</sub>(μ-Cl)(μ-Br) and for Cp<sup>+</sup><sub>4</sub>U<sub>2</sub>(μ-Cl)(μ-Br). In several cases, the barrier to ring rotation in the hetero-halide dimers was determined from the four Me<sub>3</sub>C resonances, which collapse into two resonances at temperatures similar to those observed for the homo-bridged dimers. The barriers are given in Table 3. In addition to ring rotation, another fluxional process with a higher barrier was observed in the hetero-halide dimers. At temperatures slightly above room temperature, the diastereotopic SiMe<sub>3</sub> or CMe<sub>3</sub> peaks coalesce

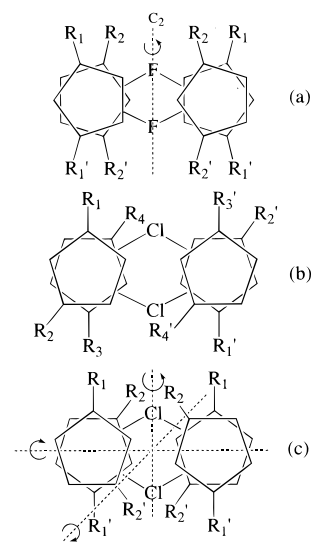


**Figure 3.** Cp'' ring conformations: (a) [Cp''<sub>2</sub>UF]<sub>2</sub>, C<sub>2h</sub> symmetry; (b) [Cp''<sub>2</sub>UCl]<sub>2</sub>, C<sub>i</sub> symmetry; (c) [Cp<sup>+</sup><sub>2</sub>UCl]<sub>2</sub>, D<sub>2</sub> symmetry.

with barriers given in Tables 4 and 5. In the Cp<sup>+</sup><sub>4</sub>U<sub>2</sub>(μ-X)(μ-Y) series, the coalescence of the A proton resonances was observed in addition to the coalescence of the CMe<sub>3</sub> resonances. The difference between the barrier determined from the A proton resonances and the barrier determined from the CMe<sub>3</sub> proton resonances varies from 0.1 to 0.2 kcal mol<sup>-1</sup>.

## Discussion

To interpret the variable-temperature <sup>1</sup>H NMR behavior of these complexes in solution, their solid-state structures must be considered. All of the [Cp''<sub>2</sub>UX]<sub>2</sub> complexes have similar structures, as shown in Figure 3, in projection to display the ring orientations clearly. While all of these complexes have crystallographically imposed inversion symmetry, [Cp''<sub>2</sub>UF]<sub>2</sub> has idealized C<sub>2h</sub> symmetry.<sup>14</sup> In [Cp''<sub>2</sub>UBr]<sub>2</sub> and [Cp''<sub>2</sub>UCl]<sub>2</sub>, the Cp'' ligands are slightly twisted, removing the 2-fold axis,<sup>6</sup> and these two compounds have idealized C<sub>i</sub> symmetry in solution. Only one of the [Cp<sup>+</sup><sub>2</sub>UX]<sub>2</sub> complexes, where X = Cl, has been crystallographically characterized;<sup>8</sup> the idealized D<sub>2</sub> symmetry of this complex is illustrated in projection in Figure 3. Presumably, [Cp<sup>+</sup><sub>2</sub>UBr]<sub>2</sub> and [Cp<sup>+</sup><sub>2</sub>UI]<sub>2</sub> have similar structures.

The solid-state structures can be used to explain the number of inequivalent SiMe<sub>3</sub> or CMe<sub>3</sub> groups observed in the low-temperature spectra. For [Cp''<sub>2</sub>UCl]<sub>2</sub> and [Cp''<sub>2</sub>UBr]<sub>2</sub>, four SiMe<sub>3</sub> resonances are observed, consistent with the C<sub>i</sub> symmetry of these dimers. For [Cp''<sub>2</sub>UF]<sub>2</sub> and [Cp<sup>+</sup><sub>2</sub>UX]<sub>2</sub> (X = Cl, Br, and I), only two SiMe<sub>3</sub> or CMe<sub>3</sub> resonances are observed, consistent with their idealized C<sub>2h</sub> and D<sub>2</sub> symmetries, respectively.

In addition to explaining the low-temperature spectra, the solid-state structures also explain the trends in the barriers to ring rotation. For [Cp<sup>+</sup><sub>2</sub>UX]<sub>2</sub> (X = Cl, Br, and I), all of the barriers to ring rotation are similar. Due to their orientation, the CMe<sub>3</sub> groups do not need to rotate past the other metallocene fragment in an in-

(14) Lukens, W. W., Jr.; Allen, P. G.; Bucher, J. J.; Edelstein, N. M.; Hudson, E.; Shuh, D.; Reich, T.; Andersen, R. A. *Organometallics* **1999**, *18*, 1253–1258.



**Figure 4.** Proposed pathway for  $\text{CMe}_3$  site exchange in  $[\text{Cp}^*_2\text{UX}]_2$  dimers.

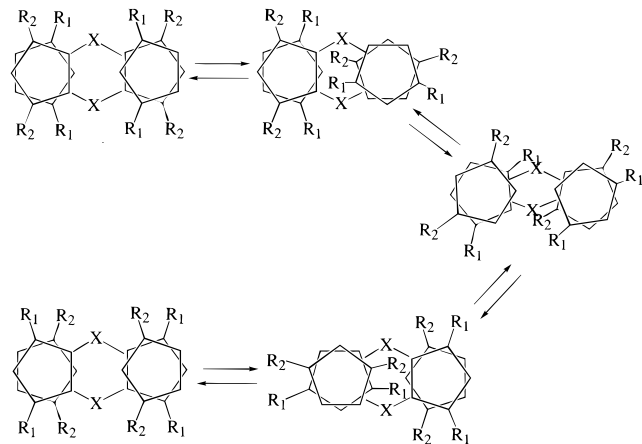


**Figure 5.** Proposed pathway for  $\text{SiMe}_3$  site exchange in  $[\text{Cp}''_2\text{UX}]_2$  dimers.

tramolecular site exchange, as illustrated in Figure 4. A  $36^\circ$  rotation of the  $\text{Cp}^+$  rings brings  $\text{R}_1$  and  $\text{R}_2$ , and  $\text{R}'_1$  and  $\text{R}'_2$ , into an eclipsed conformation with  $D_{2d}$  idealized symmetry. This process is presumably the origin of the barrier to site exchange in these complexes. Since the energy of this transition state is not greatly affected by the  $\text{U}\cdots\text{U}$  distance in the dimers, which is largely determined by the radius of the halide, the barrier should not vary much among these complexes, as observed by the values in Table 2. Among the  $\text{Cp}^+$  hetero-halide dimers, the barriers to ring rotation are, again, roughly the same as those seen in the homo-halide dimers, since the barrier should not be very sensitive to  $\text{U}\cdots\text{U}$  distance.

The  $[\text{Cp}''_2\text{UX}]_2$  ( $\text{X} = \text{F}, \text{Cl}, \text{Br}$ , and, presumably,  $\text{I}$ ) dimers all have quite similar structures. In contrast to the  $\text{Cp}^+$  dimers, the barriers to ring rotation are strongly correlated with the identity of the halide ligand, as shown in Table 2. Since the  $\text{SiMe}_3$  group must rotate past the adjacent metallocene fragment in an intramolecular site exchange, the barrier to ring rotation will be strongly affected by the  $\text{U}\cdots\text{U}$  distance. Figure 5 illustrates one possible site exchange pathway in these dimers; while other site exchange pathways may be postulated, in all cases, the  $\text{SiMe}_3$  group must rotate past the adjacent metallocene fragment. A similar explanation was used to explain the ring rotation barriers in  $(\text{Me}_3\text{CC}_3\text{H}_4)_4\text{Zr}_2(\mu\text{-O})(\mu\text{-E})$  ( $\text{E} = \text{Te}$  or  $\text{Se}$ ), in which the barrier to site exchange is correlated with the  $\text{Zr}\cdots\text{Zr}$  distance.<sup>15,16</sup> One problem with this explanation is that the  $\text{U}\cdots\text{U}$  distance in  $[\text{Cp}''_2\text{UBr}]_2$  is  $0.022 \text{ \AA}$  shorter than in  $[\text{Cp}''_2\text{UCl}]_2$ , while the barrier to ring

rotation is greater in  $[\text{Cp}''_2\text{UCl}]_2$  by about  $1 \text{ kcal mol}^{-1}$  (Table 2). However, since the  $\text{U}\cdots\text{U}$  distance in  $[\text{Cp}''_2\text{UBr}]_2$  is greater than or equal to that in the chloride dimer if the  $\text{Br}\text{-U}\text{-Br}$  angle decreases by  $1$  or  $2^\circ$  from that observed in the solid state. In the case of  $[\text{Cp}''_2\text{UF}]_2$ , the  $\text{U}\cdots\text{U}$  distance is much shorter than that in the other halide dimers; therefore, the barrier to ring rotation is greater.

Among the  $\text{Cp}''$  hetero-halide dimers, only the low-temperature spectra of the fluoride-containing dimers were amenable to interpretation. The low-temperature spectrum of  $\text{Cp}''_4\text{U}_2(\mu\text{-X})(\mu\text{-Y})$  ( $\text{X} = \text{F}, \text{Y} = \text{Br}$  or  $\text{I}$ ) is consistent with  $C_2$  symmetry and a geometry roughly the same as found for  $[\text{Cp}''_2\text{UF}]_2$ , rather than the  $C_1$  symmetry of  $[\text{Cp}''_2\text{UCl}]_2$ , as evidenced by the presence of only four inequivalent  $\text{SiMe}_3$  resonances for these complexes rather than eight. The barriers to ring rotation in these two hetero-halide-bridged complexes fall between those of  $[\text{Cp}''_2\text{UF}]_2$  and  $[\text{Cp}''_2\text{UCl}]_2$ . Since the presence of a bridging fluoride ligand in these mixed-halide dimers will result in a shorter  $\text{U}\cdots\text{U}$  distance, these site exchange barriers are, again, consistent with the assertion that the barrier is largely dictated by the  $\text{U}\cdots\text{U}$  distance, which results in the across-ring  $\text{Cp}\cdots\text{Cp}$  repulsions.<sup>16</sup>

The structure of  $[\text{Cp}^*_2\text{UF}]_2$  is not known, and the presence of six inequivalent  $\text{CMe}_3$  groups at low temperature is perplexing. Three reasons may be advanced for this observation. The complex could be a trimer with  $C_2$  symmetry as is  $[(\text{Me}_5\text{C}_5)_2\text{UCl}]_2$ .<sup>4</sup> Alternatively, the complex could exist as a mixture of rotamers, one having  $C_{2h}$  or  $D_2$  symmetry, giving two  $\text{CMe}_3$  resonances, and the other having  $C_2$ ,  $C_s$ , or  $C_i$  symmetry, giving four  $\text{CMe}_3$  resonances. Finally, the complex could have a  $C_{2h}$  structure in which the rotation of the  $\text{CMe}_3$  groups is hindered. X-ray-quality single crystals of this complex could not be obtained, but the  $\text{U}\cdots\text{U}$  distance of  $3.84 \text{ \AA}$ , determined by EXAFS, rules out the first explanation.<sup>14</sup> The oxo dimer of  $\text{U(IV)}$ ,  $[\text{Cp}^*_2\text{UO}]_2$ , has a  $C_{2h}$  structure, as determined by single-crystal X-ray crystallography,<sup>14</sup> and this compound does not show hindered rotation of the  $\text{CMe}_3$  groups down to  $-100^\circ\text{C}$ ; two inequivalent  $\text{CMe}_3$  groups are present at all temperatures. Therefore, hindered rotation of the  $\text{CMe}_3$  groups of  $[\text{Cp}^*_2\text{UF}]_2$  seems rather unlikely. The remaining explanation is that  $[\text{Cp}^*_2\text{UF}]_2$  exists as a mixture of conformers in which the  $\text{Cp}^+$  rings are locked into a specific orientation in at least two independent molecules whose molecular symmetries are different.

Even more interesting than the ring site exchange is the existence of a second fluxional process that results in the coalescence of the diastereotopic  $\text{CMe}_3$  or  $\text{SiMe}_3$  groups in the mixed-halide dimers. To make the diastereotopic groups equivalent, the complex must "gain" a mirror plane on the NMR time scale. This symmetry operation cannot be generated by ring rotation. Three processes that can make the diastereotopic groups equivalent are site exchange between the halide ligands, a change in the face of the  $\text{Cp}$  ligand that is coordinated to uranium, or dissociation of the dimer into monomers, which then recombine. The last process can be ruled out since separate resonances are observed for all three species in solution: the hetero-halide dimer and the two

(15) Erker, G.; Nolte, R.; Tainturier, G.; Rheingold, A. *Organometallics* **1989**, *8*, 454.

(16) DeKock has discussed the relative energies involved in eclipsed and staggered cyclopentadienyl rings in zirconocene dimers and how this influences the  $\text{Zr}\cdots\text{Zr}$  distance: DeKock, R. L.; Peterson, M. A.; Reynolds, L. E. L.; Chen, L.-H.; Baerends, E. J.; Vernooijs, P. *Organometallics* **1993**, *12*, 2794–2805.

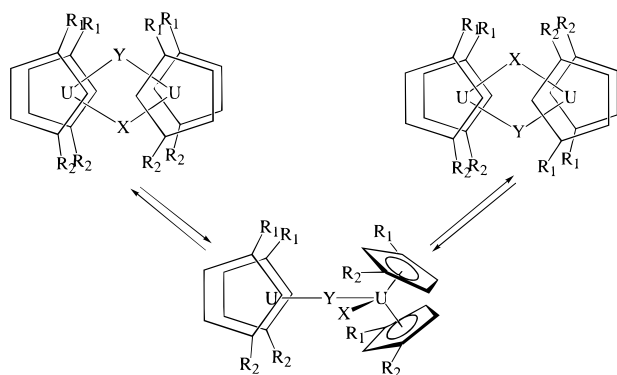


**Figure 6.** Proposed pathway for halide site exchange in hetero-halide dimers.

homo-halide dimers. If a rapid dimer–monomer equilibrium was present, only one resonance would be observed. The observation of distinct resonances shows that these complexes are dimeric at all temperatures examined and that all site exchange process must be intramolecular.

To test whether the Cp ligands could be changing coordinated faces, the variable-temperature behavior of monomeric  $\text{Cp}^{\ddagger}\text{U}(\text{Cl})(\text{Me})$  was examined. In this complex, two  $\text{CMe}_3$  resonances are observed at all temperatures, showing that the same face of the  $\text{Cp}^{\ddagger}$  ligand remains coordinated to the metal and that the Cl and Me ligands do not exchange sites to 100 °C. It is possible that both  $\text{Cp}^{\ddagger}$  ligands change faces as the Cl and Me ligands exchange sites; however, this seems highly unlikely. Thus, the likelihood of the Cp ligand changing coordinated faces is extremely small. The remaining explanation is that the halide ligands are changing sites. One possible mechanism for this exchange is shown in Figure 6. The “one-legged” transition state has precedence among  $[(\text{Me}_5\text{C}_5)_2\text{MX}]_2$  dimers where  $\text{X} = \text{Cl}$  and  $\text{M} = \text{Y}$ <sup>17</sup> and where  $\text{X} = \text{Me}$  and  $\text{M} = \text{Y}$ ,<sup>18</sup> Lu,<sup>18</sup> and Yb.<sup>19</sup> Note that, in the process shown in Figure 6, the halides exchange sites on only one monomer unit (the left one), so that the process occurs at twice the rate determined from the NMR spectra. This doubling of the rate decreases the site exchange barriers in Tables 4 and 5 by 0.4 kcal mol<sup>-1</sup>.

The values in Tables 4 and 5 for the hetero-halide-bridged metallocene complexes are consistent with the postulate that the larger halide is the bridging halide in the “one-legged” transition state, since the barriers are smallest when the complex contains F or I. The U–F bond is the shortest; therefore, a terminal fluoride ligand will have the smallest steric interaction with the other metallocene unit in the transition state. Because the U–I bond is the longest, the metallocene units will be furthest apart with a bridging iodide in the transition state, thereby minimizing intramolecular steric interactions.

In conclusion, the solution behavior of the  $[\text{Cp}^{\ddagger}_2\text{UX}]_2$  and  $[\text{Cp}^{\ddagger\prime}_2\text{UX}]_2$  complexes has been examined. These complexes exist as dimers throughout the temperature range examined. The barriers to ring rotation are

largely dictated by the  $\text{U}\cdots\text{U}$  distance in the  $[\text{Cp}^{\ddagger\prime}_2\text{UX}]_2$  dimers and by the energy of the eclipsed conformation in the  $[\text{Cp}^{\ddagger}_2\text{UX}]_2$  dimers. The hetero-halide dimers show coalescence of the resonances due to diastereotopic  $\text{CMe}_3$  or  $\text{SiMe}_3$  groups by a physical process that is thought to involve intramolecular halide site exchange by way of a “one-legged” intermediate.

### Experimental Details

All reactions and manipulations were carried out under an inert atmosphere using standard Schlenk and drybox techniques; the experimental procedures have been described previously.<sup>9</sup> Unless otherwise noted, <sup>1</sup>H NMR spectra were acquired in benzene-*d*<sub>6</sub> using a JEOL FX-90Q spectrometer operating at 89.56 MHz; the chemical shifts of the resonances are listed in Table 1.  $\text{Cp}^{\ddagger}_2\text{UCl}_2$ ,  $\text{Cp}^{\ddagger}_2\text{UBr}_2$ , and  $\text{Cp}^{\ddagger}_2\text{UI}_2$  were made by a variation of the published procedures.<sup>9,20</sup>  $[\text{Cp}^{\ddagger}_2\text{UF}]_2$ ,  $[\text{Cp}^{\ddagger}_2\text{UCl}]_2$ ,  $[\text{Cp}^{\ddagger}_2\text{UBr}]_2$ , and  $[\text{Cp}^{\ddagger}_2\text{UI}]_2$  have been reported previously.<sup>6</sup>

**$[\text{Cp}^{\ddagger}_2\text{UF}]_2$ .**  $\text{Cp}^{\ddagger}_2\text{UF}_2$ <sup>9</sup> (1.68 g, 2.66 mmol) was dissolved in 50 mL of hexane, and *t*-BuLi (1.5 mL, 1.85 M in hexane, 2.8 mmol) was added using a syringe. The solution immediately turned green and cloudy. After the mixture was stirred for 12 h, the hexane was removed under reduced pressure. The green solid residue was suspended in 100 mL of toluene and heated to 60 °C. The mixture was cooled to room temperature and filtered, and the volume of the filtrate was reduced to ca. 25 mL. Cooling to –20 °C produced small, dark green crystals (0.79 g). The volume of the mother liquor was reduced to ca. 10 mL, and cooling to –20 °C yielded another crop of green solid (combined yield 1.10 g, 68%). The compound did not melt to 300 °C. IR: 3067 (w), 1304 (w), 1291 (w), 1252 (s), 1234 (w), 1201 (m), 1163 (m), 1055 (m), 1021 (m), 925 (m), 817 (m), 799 (s), 743 (s), 676 (m), 659 (m), 610 (w), 435 (w), 330 (s) cm<sup>-1</sup>. MS ( $\text{M}^+$  *m/z*) (calcd, found): 1223 (100, 100), 1224 (58, 56), 1225 (17, 16). Anal. Calcd for  $\text{C}_{26}\text{H}_{42}\text{FU}$ : C, 51.1; H, 6.92. Found: C, 50.8; H, 6.87.

**$[\text{Cp}^{\ddagger}_2\text{UF}]_2$ .**  $[\text{Cp}^{\ddagger}_2\text{UF}_2]$ <sup>9</sup> (1.59 g, 2.29 mmol) was dissolved in 50 mL of hexane, and *t*-BuLi (1.30 mL, 1.85 M in hexane, 2.40 mmol) was added using a syringe. The solution instantly turned dark green. After the mixture was stirred for 8 h, the hexane was removed under reduced pressure, giving a dark green solid. The green solid residue was suspended in 50 mL of hexane, and the mixture was filtered. The volume of the filtrate was reduced to ca. 10 mL. Cooling to –20 °C produced dark green blocks (0.46 g, 30%). Mp: 244–246 °C. IR: 3040 (w), 1316 (w), 1249 (s), 1205 (w), 1076 (s), 1055 (w), 919 (s), 836 (s), 773 (m), 752 (s), 691 (m), 635 (m), 621 (w), 475 (m), 370 (m), 330 (s), 300 (m), 280 (w), 240 (w) cm<sup>-1</sup>. MS ( $\text{M}^+$  *m/z*) (calcd, found): 1347 (100, 100), 1348 (90, 87), 1349 (66, 60), 1350 (34, 41), 1351 (15, 23), 1352 (5, 12). Anal. Calcd for  $\text{C}_{22}\text{H}_{42}\text{FSi}_4\text{U}$ : C, 39.1; H, 6.26. Found: C, 37.8; H, 6.17.

**$[\text{Cp}^{\ddagger}_2\text{UCl}]_2$ .** A solution of  $\text{Cp}^{\ddagger}_2\text{UCl}_2$ <sup>9</sup> (2.00 g, 3.01 mmol) in 100 mL of hexane was cooled to –80 °C, and *t*-BuLi (1.6 mL, 1.9 M in hexane, 3.01 mmol) was added by syringe. The mixture was warmed to room temperature with stirring. After 3 h, the hexane was removed under reduced pressure. The green solid residue was extracted with 2 × 30 mL of toluene, and the mixture was filtered. The volume of the filtrate was reduced to ca. 50 mL. Cooling to –80 °C gave dark green blocks (1.2 g, 63%). The compound did not melt to 310 °C. IR: 3070 (w), 2820 (w), 1295 (w), 1250 (s), 1230 (w), 1205 (m), 1165 (m), 1055 (m), 1025 (m), 930 (m), 815 (m), 805 (s), 765 (m), 750 (s), 720 (w), 675 (m), 660 (m), 610 (w), 425 (w), 345 (m) cm<sup>-1</sup>. MS ( $\text{M}^+$  *m/z*) (calcd, found): 1255 (100, 100), 1256 (58, 60), 1257 (81, 50), 1258 (41, 26). Anal. Calcd for  $\text{C}_{26}\text{H}_{42}\text{ClU}$ : C, 49.7; H, 6.69. Found: C, 49.8; H, 6.76.

(17) Evans, W. J.; Peterson, T. T.; Rausch, M. D.; Hunter, W. E.; Zhang, H.; Atwood, J. L. *Organometallics* **1985**, *4*, 554–559.

(18) Watson, P. L. *J. Am. Chem. Soc.* **1983**, *105*, 6491–6493.

(19) Matsunaga, P. T., Ph.D. Thesis, University of California, Berkeley, 1991.

(20) Blake, P. C.; Lappert, M. F.; Taylor, R. G. *Inorg. Synth.* **1990**, *27*, 172.

**[Cp''<sub>2</sub>UCI]<sub>2</sub>**.<sup>6</sup> Cp''<sub>2</sub>UCl<sub>2</sub><sup>20,9</sup> (2.00 g, 2.75 mmol) was dissolved in 50 mL of hexane, and *t*-BuLi (1.14 mL, 2.4 M in hexane, 2.8 mmol) was added by syringe. The solution quickly turned green. After it was stirred for 12 h, the mixture was heated to 80 °C and filtered. The green solid residue was washed with 50 mL of hexane, which was added to the filtrate. The volume of the combined filtrate was reduced to ca. 40 mL, and the filtrate was heated to 80 °C to dissolve the solid. Cooling to -80 °C produced green blocks (1.25 g, 66%). IR: 1310 (w), 1245 (s), 1200 (w), 1070 (s), 915 (s), 830 (s), 780 (w), 775 (w), 745 (s), 685 (m), 630 (m), 615 (m), 480 (m), 365 (m), 350 (w), 330 (3), 300 (m), 280 (w) cm<sup>-1</sup>. MS weak peak for (M)<sup>+</sup> *m/z* (calcd, found): 1382 (77, 100), 1384 (100, 97). Anal. Calcd for C<sub>22</sub>H<sub>42</sub>-ClSi<sub>4</sub>U: C, 38.2; H, 6.11; Cl, 5.12. Found C, 37.9; H, 6.11; Cl, 5.28.

**[Cp''<sub>2</sub>UBr]<sub>2</sub>**. Cp''<sub>2</sub>UBr<sub>2</sub><sup>9</sup> (0.52 g, 0.69 mmol) was dissolved in 30 mL of diethyl ether, and *t*-BuLi (0.29 mL, 2.4 M in hexane, 0.70 mmol) was added by syringe. The initially red solution immediately became bright green. After the mixture was stirred for 2 h, the solvent was removed under reduced pressure, and the green solid residue was suspended in 30 mL of hexane. The mixture was filtered, and the volume of the filtrate was reduced to ca. 20 mL. Cooling to -80 °C gave green needles (0.25 g, 54%). The compound did not melt to 300 °C. MS (M)<sup>+</sup> *m/z* (calcd, found) 671 (98, 100), 672 (29, 28), 673 (100, 100), 674 (29, 26). Anal. Calcd for C<sub>26</sub>H<sub>42</sub>BrU: C, 46.4; H, 6.3; Br, 11.9. Found: C, 46.6; H, 6.40; Br, 12.0.

**[Cp''<sub>2</sub>UBr]<sub>2</sub>**.<sup>6</sup> Cp''<sub>2</sub>UBr<sub>2</sub><sup>9,20</sup> (0.75 g, 0.92 mmol) was dissolved in 50 mL of hexane, and *t*-BuLi (0.38 mL, 2.4 M in hexane, 0.91 mmol) was added by syringe. The solution slowly became green and cloudy. After it was stirred for 7 h, the mixture was heated to 60 °C and allowed to settle. The mixture was filtered, and the volume of the filtrate was reduced to ca. 15 mL. Cooling to -80 °C produced small green blocks (0.45 g, 66%). The compound did not melt to 250 °C. IR: 3070 (w), 3020 (w), 1325 (m), 1245 (s), 1200 (m), 1075 (s), 915 (s), 830 (s), 785 (m), 775 (w), 750 (s), 690 (m), 635 (s), 615 (m), 475 (m), 370 (m), 350 (w), 330 (w), 300 (m), 280 (w), 240 (w) cm<sup>-1</sup>. MS (M)<sup>+</sup> *m/z* (calcd, found): 1470 (38, 44), 1471 (34, 50), 1472 (100, 100),

1473 (80, 94), 1474 (91, 94), 1475 (61, 60), 1476 (56, 33). Anal. Calcd for C<sub>22</sub>H<sub>42</sub>BrSi<sub>4</sub>U: C, 35.9; H, 5.74; Br, 10.8. Found: C, 35.9; H, 5.84; Br, 10.7.

**[Cp''<sub>2</sub>UI]<sub>2</sub>**. Cp''<sub>2</sub>UI<sub>2</sub><sup>9</sup> (0.65 g, 0.77 mmol) was dissolved in 60 mL of hexane, and *t*-BuLi (0.32 mL, 2.4 M in hexane, 0.77 mmol) was added by syringe. After 8 h of stirring, the green, cloudy mixture was heated to 60 °C for 30 min and then cooled to room temperature and filtered. The volume of the filtrate was reduced to ca. 20 mL. Cooling to -80 °C produced green needles (0.26 g, 47%). Mp: 273–278 °C. IR: 3070 (w), 2720 (w), 1295 (w), 1250 (w), 1200 (m), 1165 (m), 1050 (m), 1020 (m), 925 (m), 815 (s), 805 (s), 765 (m), 750 (s), 675 (m), 655 (m), 425 (w), 345 (w) cm<sup>-1</sup>. MS (M)<sup>+</sup> *m/z* (calcd, found): 719 (100, 100), 720 (30, 30), 721 (4, 5). Anal. Calcd for C<sub>26</sub>H<sub>42</sub>IU: C, 43.4; H, 5.88. Found: C, 43.4; H, 5.94.

**[Cp''<sub>2</sub>UI]<sub>2</sub>**.<sup>6</sup> Cp''<sub>2</sub>UI<sub>2</sub><sup>20,9</sup> (1.00 g, 1.10 mmol) was dissolved in 50 mL of hexane, and *t*-BuLi (0.62 mL, 1.85 M in hexane, 1.1 mmol) was added by syringe. The solution became green and cloudy. After the mixture was stirred for 12 h, 25 mL of hexane was added, and this mixture was heated to 60 °C. The mixture was filtered, and the volume of the filtrate was reduced to ca. 30 mL. Cooling to -80 °C produced green blocks (0.74 g, 88%). The compound did not melt to 250 °C. IR 1320 (w), 1245 (s), 1200 (w), 1175 (s), 915 (s), 830 (s), 790 (w), 780 (w), 750 (m), 960 (w), 645 (m), 615 (w), 475 (m), 375 (w), 350 (w), 200 (w) cm<sup>-1</sup>. MS (M)<sup>+</sup> *m/z* (calcd, found): 1566 (100, 100), 1567 (90, 82), 1568 (66, 57), 1569 (34, 37), 1570 (15, 12). Anal. Calcd for C<sub>22</sub>H<sub>42</sub>ISi<sub>4</sub>U: C, 33.7; H, 5.40; I, 16.2. Found: C, 33.5; H, 5.29; I, 16.2.

**Acknowledgment.** This work was partially supported by the Director, Office of Energy Research, Office of Basic Energy Sciences, Chemical Sciences Division, of the U.S. Department of Energy under Contract No. DE-AC03-76SF00098. W.W.L. thanks the National Science Foundation for a graduate fellowship.

OM9805990